Journal of Fluorine Chemistry 134 (2012) 18–23

Contents lists available at ScienceDirect

Journal of Fluorine Chemistry

journal homepage: www.elsevier.com/locate/fluor

Fluoride and oxyfluoride glasses for optical applications

V. Nazabal [a,*], M. Poulain [a,*], M. Olivier [a], P. Pirasteh [a], P. Camy [b], J.-L. Doualan [b], S. Guy [c], T. Djouama [e], A. Boutarfaia [d], J.L. Adam [a]

[a] Sciences Chimiques de Rennes, UMR-CNRS 6226, Equipe Verres et Céramiques, Université de Rennes1, 35042 Rennes, France
[b] CIMAP, ENSI Caen, 6 boulevard du Maréchal Juin, 14050 Caen cedex 4, France
[c] Laboratoire de Physico-Chimie des Matériaux Luminescents (LPCML), UMR-CNRS 5620, Université Claude Bernard-Lyon 1, Villeurbanne, France
[d] Laboratoire de Chimie Appliquée, Université M. Khider, 07000 Biskra, Algeria
[e] Laboratoire d'Électronique Quantique, Faculté de Physique, USTHB. BP 32, El-Alia 16111, Alger, Algeria

ARTICLE INFO

Article history:
Received 14 January 2011
Received in revised form 26 June 2011
Accepted 28 June 2011
Available online 5 July 2011

Keywords:
Fluoride and oxyfluoride glasses
Channeled waveguide
Compact laser source

ABSTRACT

This paper present some recent developments on fluoride and oxyfluoride glasses, including glass composition, basic characterizations, technology and prospects, especially the development of rare earth doped fluoride glass channel waveguides for applications requiring integrated optical components. New Heavy Metal Fluoride Glasses compositions have been investigated namely manganese-rich fluorozirconates and strontium fluorohafnates. Numerous fluorophosphate glasses have also been obtained by the incorporation of $NaPO_3$ and Na_2PO_3F in the unstable MnF_2–BaF_2 and NbO_2F–BaF_2 binary glasses. NMR and electrical conductivity measurements were conducted on these glasses. Rare earth-doped channeled planar waveguides were made from the rare earth doped ZBLA ($57\%ZrF_4$–$34\%BaF_2$–$(5-x)\%LaF_3$–$4\%AlF_3$–$x\%REF_3$) glass by ionic exchange using optical lithography. The spectroscopic properties of Pr^{3+} doped ZBLA planar waveguides were investigated by comparison to bulk samples. For Er^{3+}/Ce^{3+} doped ZBLA channeled waveguide low background losses (0.3 dB/cm) and net gain in excess of 1 dB/cm at 1.5 μm were obtained for incident pump powers higher than 200 mW.

1. Introduction

While the discovery of the first fluorozirconate glasses in 1974 was serendipitous [1], these glasses have attracted a large attention in the glass community. These glasses have been the subject of numerous studies [2–5]. Their intrinsic physical properties – high transparency and low phonon energy – make them attractive materials for a set of photonic applications [5,6]. These applications have been developed in the framework of telecommunication technologies, where silica fibers reached their limits. This is the case for optical transmission in the mid-infrared beyond 2 μm, and active fibers for which low phonon energy is required. Taking into consideration that the most stable among the heavy metal fluoride glasses (HMFG) easily doped by rare-earth ions is the ZBLAN (ZrF_4–BaF_2–LaF_3–AlF_3–NaF), it has been extensively studied for efficient ultraviolet, visible, and infrared fiber lasers [7,8]. While early developments focused on telecommunications, fluoride glass fibers are actually scarcely used in this field, with only a few optical amplifiers available. They made possible the coupling of large telescopes, leading to an unprecedented resolution [9]. Current applications encompass remote spectroscopy, thermometry, IR imaging and laser power delivery. Fiber lasers based on HMFG offer a large potential, with numerous emission lines. Especially promising are compact fiber lasers operating around 2.9 μm with CW output power in excess of 10 W [10]. HMFG supercontinuum sources are now available in a broad spectral range, between 800 nm and 4 μm or beyond. They are likely to promote innovative devices for spectral analysis and counter-measurements. Also, the last 10 years have seen a high demand for integrated optical systems to be implemented in high-bit-rate local and metropolitan networks for the telecommunication field, for which the development of optoelectronic components with small dimensions after packaging and low cost was required. A context of basic needs for visible laser sources come into being to meet the demand for lighting application and quantum information processing. The main interest of fluoride microguiding structures, over fiber and semiconductor, lies in the possibility to integrate simultaneously on a same small substrate a great number of optical functions, like amplification related to wavelength division multiplexing (WDM) or laser to realize compact solid state laser sources emitting in the visible range and linked with couplers, multiplexers or detectors.

One of the attractive features of fluoride glasses lies in their predominant ionicity, which makes them a specific group. Fluoride

* Corresponding authors.
E-mail addresses: virginie.nazabal@univ-rennes1.fr (V. Nazabal), marcel.poulain@univ-rennes1.fr (M. Poulain).

0022-1139/$ – see front matter © 2011 Elsevier B.V. All rights reserved.
doi:10.1016/j.jfluchem.2011.06.035

glass technology has outlined some common features, such as the chemical reactivity of fluoride melts, devitrification tendency and sensitivity to water. Most of the associated problems could be solved or partly controlled. In that sense, oxyfluoride glasses, especially fluorophosphate glasses, make a compromise between oxide and fluoride materials.

This paper intends to make the overview of the current researches at Rennes University where first HMFG were synthesized. To this end, this article summarized the research activity of the last 5 years that concerns both the development of new fluoride glass composition and the glass shaping with the manufacture of optical waveguide in fluoride glass by ion exchange. This paper describes the different studied glass compositions, their basic physico-chemical characterizations, technology and prospects, especially the development of (Pr^{3+} or Er^{3+}/Ce^{3+})-doped ZBLA glass channel waveguides for applications requiring integrated optical components. Low phonon energy materials doped with rare earth ions such as Pr^{3+} can be used to realize compact solid state laser sources emitting in the visible range. Indeed, the direct pumping of the Pr^{3+} ion, in which a blue photon is converted to a green or a red photon, is a very attractive solution, since it is a simple way to obtain the population inversion. The study of a new generation of erbium-doped waveguide amplifiers is responding to the problem of access in metropolitan networks and satisfying the criteria of broadband and high-speed connection created by wavelength division multiplexing. The originality of this work lies in the use of fluoride glasses which enables to expect a flat gain bandwidth around 1.55 μm.

2. Materials and methods

2.1. Synthesis of fluoride and oxyfluoride glasses

2.1.1. Preparation

Glass synthesis includes a series of classical steps: mixing of starting materials, melting, fining, casting and annealing. Glass samples are prepared according to a method reported elsewhere [11]. High-purity chemical reagents and very dry atmosphere are required for manufacturing optical fibers and optical quality glass samples. Thus, the glass batches were prepared from reagent grade >99.9% fluorides stored and handled in a dry box to prevent hydroxide and oxide contamination (H_2O = 2 ppm, O_2 = 0.5 ppm). Depending on glass stability, cooling rate must be adjusted to prevent crystallization upon cooling.

2.1.2. Composition

HMFG encompass three major families: fluoroaluminates, fluorozirconates and fluoroindates based respectively on AlF_3, ZrF_4 and InF_3 as glass progenitors and major components. They are multicomponent glasses as binary or ternary glasses exhibit large crystallization rates. Table 1 reports standard compositions. Typical glasses were defined in the AlF_3–BaF_2–YF_3–CaF_2, ZrF_4–BaF_2–LaF_3–AlF_3–NaF and InF_3–SrF_2–BaF_2–SrF_2 systems. In most cases, zirconium and indium may be replaced by hafnium and gallium. The glass composition was checked using scanning electron microscopy with an energy-dispersive X-ray analyzer. (Er^{3+}, Ce^{3+} and Pr^{3+}) rare earth and F^- ion concentrations in doped-glass samples were determined by inductively coupled plasma mass spectrometry (ICP-MS) and specific electrode method, respectively.

Table 1
Chemical composition of typical heavy metal fluoride glasses.

Glass	Composition (mol.%)
ZBNA	52ZrF_4, 24BaF_2, 20NaF, 4AlF_3
ZBLA	57ZrF_4, 34BaF_2, 5LaF_3, 4AlF_3
ZBLAN	53ZrF_4, 20BaF_2, 3LaF_3, 4AlF_3, 20NaF
YABCS	16YF_3, 40AlF_3, 12BaF_2, 22CaF_2, 10SrF_2
IBSZC	36InF_3, 15BaF_2, 20SrF_2, 20ZnF_2, 5CaF_2
PGICZ	30PbF_2, 20GaF_3, 15InF_3, 20CdF_2, 15ZnF_2
ZFG8	35ZrF_4, 20HfF_4, 25BaF_2, 3LaF_3, 3AlF_3, 14NaF

2.1.3. Properties

Glass transition temperature T_g is lower in HMFG than in oxide glasses. Typically, it ranges from 200 °C to 400 °C, while liquidus temperature T_l – at which crystal growth rate is nil – lies usually between 550 °C and 700 °C. Thermal properties were measured by differential scanning calorimetry with heating rate of 10 K/min (accuracy ±2 K). In these conditions, the temperature for fiber drawing is below 500 °C. Standard glass characterizations also include crystallization temperature that is observed between T_g and T_l. The resistance to devitrification in the molten state depends critically on chemical composition. Thermal expansion ranges from 140 to 220 10^{-7} K^{-1} [5]. These large values make HMFG rather sensitive to thermal shocks. The density of samples was determined using a helium picnometer, with ±0.004 g/cm^3 accuracy. It usually ranges from 4 to 7 g cm^{-3}.

2.2. Channeled waveguide fabrication

After the tricky polishing step, the substrates were patterned using optical lithography. A positive photoresist was spin-coated onto the SiO_2-coated ZBLA substrates. A dry etching of the SiO_2 thin film is performed in a RIE system with pure CF_4 plasma or an O_2 and CHF_3 gas mixture leading to a highly anisotropic profile and negligible contamination of the ZBLA material. During ion exchange process, the samples are set in an alumina tube, which is subject to an inert gas flow (Ar) before and after the treatment. The samples are exposed to an Argon (2 l h^{-1})-diluted HCl gas flow (2 l h^{-1}) during the exchange process and then to a HF gas flow for passivation of the surface exchanged.

2.3. Optic and spectroscopic characterization

Transmittance spectra of RE:ZBLA glasses (RE: Er^{3+}, Ce^{3+} or Pr^{3+}) were measured at room-temperature from 250 to 3200 nm using a spectrophotometer. The refractive indices of the glasses and exchanged layers were determined using different laser beam wavelengths (633, 825, 1311 and 1551 nm) by measuring the critical angle for the sample/prism interface (accuracy ±0.001) and by M-Lines allowing also the determination of the exchanged layer thickness, respectively. The waists of the channels were determined by near-field optical characterization. A lock-in amplifier, a monochromator and a photomultiplier tube were used to detect emission spectra for which a blue laser diode operating at 442 nm was employed as excitation source of Pr^{3+}. Fluorescent decays were measured using the pulsed excitation of a YAG:Nd-pumped optical parametric oscillator laser emitting at around 442 nm. A pump laser (1.48 μm fiber diode) that delivers a maximum output power of 400 mW was used for gain measurement of Er^{3+}/Ce^{3+} co-doped ZBLA channeled waveguide. The two laser beams are coupled by means of a multiplexer (MUX). Two interferential filters around 1.54 μm (transmission bandwidth of 1 nm) were placed in front of the Ge detectors.

3. Results and discussions

3.1. Rare earth doped fluoride glasses for planar waveguides

3.1.1. Glass synthesis and exchange treatment

Table 2 sums up the results for ZBLA glass of the investigated physicochemical and optical properties such as density, glass transition temperature, composition, transmission and refractive

Table 2
Physicochemical and optical properties of ZBLA glasses.

ZBLA glass	
Composition	$57ZrF_4$–$34BaF_2$–$(5-x)$ LaF_3–$4AlF_3$–$xPrF_3$
T_g	316 °C ± 2 °C
n (633 nm)	1.517 ± 0.001
Cauchy distribution	$n = 1.506 + 5.55 \times 10^3 \lambda^{-2} + -4.10 \times 10^8 \lambda^{-4}$
Transmission	0.2 μm → 7 μm
Phonon energy	575 cm^{-1}
Density	4.600 ± 0.004 g cm^{-3}
Coefficient of thermal expansion	$17.3 \times 10^{-6} K^{-1}$
Hardness	2542 MPa

Table 3
Pr^{3+}:ZBLA glass composition analyzed by ICP and specific electrode.

Ion	Theoretical atomic %	Measured atomic %
F	76.36	76.05 ± 0.84
Zr	13.48	13.44 ± 0.27
Ba	8.04	7.93 ± 0.16
La	1.06	0.90 ± 0.05
Al	0.95	1.87 ± 0.10
Pr	0.12	0.10 ± 0.01

index. The analyzed concentration is in good agreement with the theoretical composition with a slight decrease of aluminum content (Table 3). ZBLA glasses (undoped or doped with Er^{3+}/Ce^{3+} or Pr^{3+}) were used as substrate with appropriate properties and optical homogeneity to enable waveguide fabrication. In order to produce a light-guiding structure, the ion exchange process should lead to a refractive index increase at the surface of the sample [12–14]. A secondary ion mass spectroscopy (SIMS) analysis was used to characterize the composition of the glass and has clearly demonstrated the presence of Cl^- ions on a few microns into the fluoride glass. After the exchange treatment, the concentration profile of chloride ion has a plateau more or less wide (few microns) then a steep drop followed by a gentle decline, related to a classical diffusion of Cl^- ions in the glass over several microns (maximum 10 μm) until the initial composition of the glass is reached again. The influence of the temperature of ionic exchange treatment has been evaluated following the evolution of refractive index and layer thickness on the exchanged planar waveguides (Fig. 1). For the same treatment time, the thickness of the exchanged layer increases with temperature. Indeed, higher temperature allows better diffusion of chloride ions in the vitreous

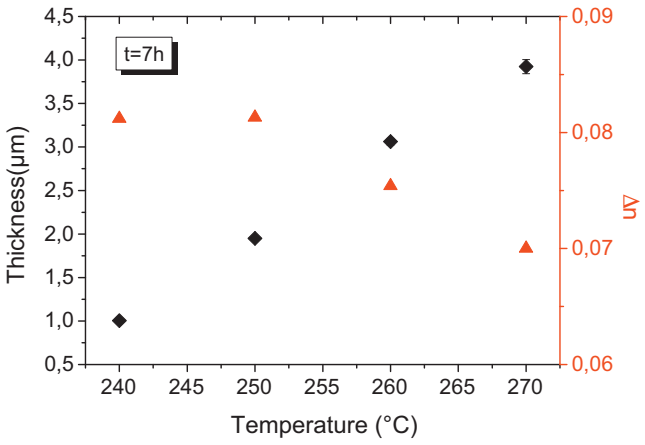

Fig. 1. Influence of the temperature of ionic exchange process on the exchanged layer thickness and refractive index difference between the exchanged layer and the Pr^{3+}:ZBLA glass substrate (treatment duration fixed at 7 h).

Table 4
Refractive index (n), thickness (e) and number of guided modes obtained at 633 nm for different parameters of ion exchange process.

t (h)	T (°C)	e (μm)	n (±0.001) at 633 nm	Number of guided modes
5	250	1.44	1.596	3
5	260	2.92	1.592	5
7	240	1.36	1.597	3
7	250	2.24	1.598	3
7	260	3.16	1.593	6
9	260	3.68	1.595	7

matrix. Refractive index and number of guided modes at 633 nm are determined by the M-lines method and are summarized for the case of Pr^{3+}:ZBLA glasses in Table 4. For these samples, the refractive index variation (Δn) obtained is about 0.08. The variation is large enough to achieve optical waveguiding in the visible range. The thickness of the guiding core, near 4 μm, may be still increased by adjusting the post-diffusion time. This will also allow controlling the refractive contrast between the non-exchanged bulk glass and the exchanged layer.

3.1.2. Spectroscopic measurements

3.1.2.1. Pr^{3+} co-doped ZBLA channel waveguides. Spectroscopic studies have been performed to optimize the rare-earth doping level in order to reach the best compromise ensuring good optical quality, highest lifetime and efficient emission intensity at 635, 605 and 520 nm. The transitions from the $^3H_4$ ground level to the $^3P_0$, $^1I_6$/$^3P_1$, $^3P_2$ and $^1D_2$ manifolds were identified. It is interesting to point out the relatively broad, most intense, band around 442 nm in the absorption spectrum, which is suitable for a direct pumping with a GaN blue laser diode. The typical emission transitions of praseodymium ions in the visible can be observed around 636, 604, 536, 521 and 480 nm. These emission lines are associated with transitions from the thermalized $^3P_1$, $^1I_6$ and $^3P_0$ levels to the $^3H_5$, $^3H_6$ and $^3F_2$ levels, around 521/536, 604, and 636 nm, respectively [15,16].

Fluorescence decays of $^3P_0$ level measurements were performed on ZBLA glasses with several Pr^{3+} concentrations ranging from 0.1 to 3 mol.%. The values for the fluorescence lifetimes measured at room temperature are found between 43 ± 2 μs and 12 ± 1 μs and the longest lifetime is obtained for a Pr^{3+} concentration of 0.2 mol.%. Such behavior of the fluorescence decay with concentration is likely due to energy transfer; cross-relaxation between active Pr^{3+} ions in $^3P_0$ excited state level and $^3H_4$ ground state. For laser application, we selected a Pr^{3+} concentration of 0.5 mol.% to have enough pump absorption on several millimeters samples and a lifetime of about 37 μs which compares well with Pr^{3+}:crystals. Optical measurements were also performed on an ion-exchanged glass sample corresponding to a planar waveguide having a thickness of about 3.7 μm pumped by the 442 nm signal and the resulting fluorescence was collected at the waveguide output. Fig. 2 shows the fluorescence emitted by the exchanged layer acting as a planar waveguide. Indeed, its refractive index is sufficiently higher than that of the glass, obeying the rules governing the modes propagation. Channel waveguides have been characterized using a blue laser diode emitting at 442 nm with an input power from 80 to 250 mW. Dimensions of the guides were about 4 μm depths, and between 2 and 10 μm widths for a length of 15 mm. Fluorescence and guiding properties have been easily observed on several waveguides. The emission spectrum of the planar waveguide was compared to that of a bulk sample normalized at 633 nm, which is at a wavelength for which reabsorption does not occur. A slight broadening, most likely due to the presence of Cl^- ions in the exchanged layer, can be observed, but the overall spectrum, and its relative intensities were similar. Gain and optical losses

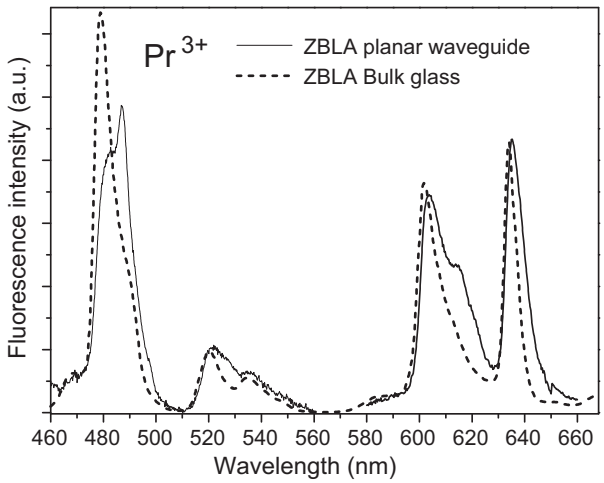

Fig. 2. Fluorescence from a Pr^{3+}:ZBLA ion exchange waveguide compared to bulk emission.

measurement are currently under progress as well as the modelization of laser effect in Pr^{3+}-doped ZBLA matrix.

3.1.2.2. Er^{3+}/Ce^{3+} co-doped ZBLA channel waveguides. In the conventional band (C-band), Er^{3+}–doped fluoride glass fiber amplifiers were of interest because an intrinsic flat gain response can be expected, as compared to silica-based amplifiers. The high-refractive-index region of the guiding structure was induced by substituting chloride for fluoride ions in the few microns under the surface of the ZBLA glass and fluoride glass channel waveguides were then obtained by means of this original ion-exchange process associated to photolithography techniques. The resulting Er^{3+}/Ce^{3+} co-doped ZBLA channel waveguides are slightly elliptical because of the nearly isotropic diffusion of the Cl^- ions during the ionic exchange process (Fig. 3). The mean $1/e^2$ waists of these waveguides measured at 1.55 μm were equal to 8.5/7.3 μm and 12.1/8.7 μm, respectively, in the *x* and *y* directions related to the two window widths of a lithography mask (3 and 5 μm). All the waveguides are single mode at 1.55 μm and the propagation losses are low with a superior limit of 0.30 dB/cm determined by double-pass technique [17], which is promising for the realization of optical amplification. The on–off gain for the return pass for which

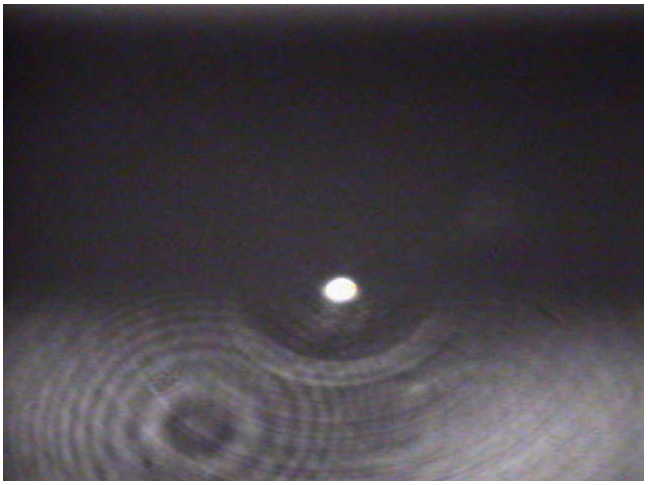

Fig. 3. Near-field image at the output of the waveguide recorded at 1.55 μm, a single-mode waveguide of 5 μm width obtained by ionic exchange treatment at 280 °C during 3 h30 for HCl gas followed by 5 h for HF gas.

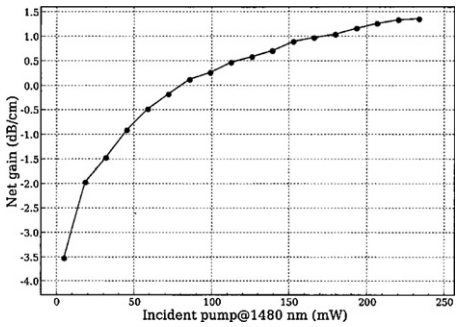

Fig. 4. Gain values under 1.48 μm pumping on a ZBLA:Er/Ce codoped waveguide, performed with the double-pass technique. The gain is measured on the return pass for which launching efficiency is maximized. The signal power at 1.54 μm is equal to −40 dBm [17].

the coupling losses were minimized by use of a second detector. The net gain was then calculated The evolution of the net gain as a function of incident pump power measured on a ZBLA:Er^{3+}/Ce^{3+} codoped waveguide is presented in Fig. 4. For the first time to our knowledge, a net gain was obtained greater than 1 dB/cm for incident pump powers higher than 250 mW.

3.2. New fluoride glass composition

Numerous glass forming systems based on pure fluorides have been investigated so far. Additional research aims either at fundamental purposes or at specific requirements. One of these is the IR transmission at longer wavelength. In this respect, glasses based on manganese difluoride are expected to have a larger IR cut-off wavelength than the other standard fluoride glasses. Glass formation has been studied in the ZrF_4–BaF_2–MnF_2 ternary system [18], as reported in Fig. 5. There are two vitreous areas in this system, which exemplifies the vitrifying ability of MnF_2. Glasses close to the binary composition are more transparent than ZBLAN in the IR spectrum. Unfortunately, their maximum thickness is limited by their devitrification tendency. The evolution of the physical properties as a function of composition has been studied by the implementation of the AlF_3/ZnF_2, MnF_2/ZrF_4, MnF_2/AlF_3 and MnF_2/BaF_2 substitutions. Glass transition temperature is close to 300 °C and the position of the infrared absorption edge is consistent with early studies on HMFGs. These new glasses are attractive materials for magnetic and photosensitivity studies.

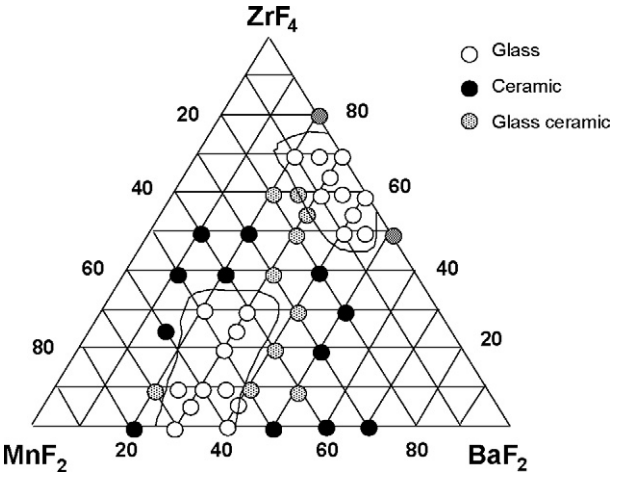

Fig. 5. Glass forming area in the ZrF_4–BaF_2–MnF_2 ternary systems.

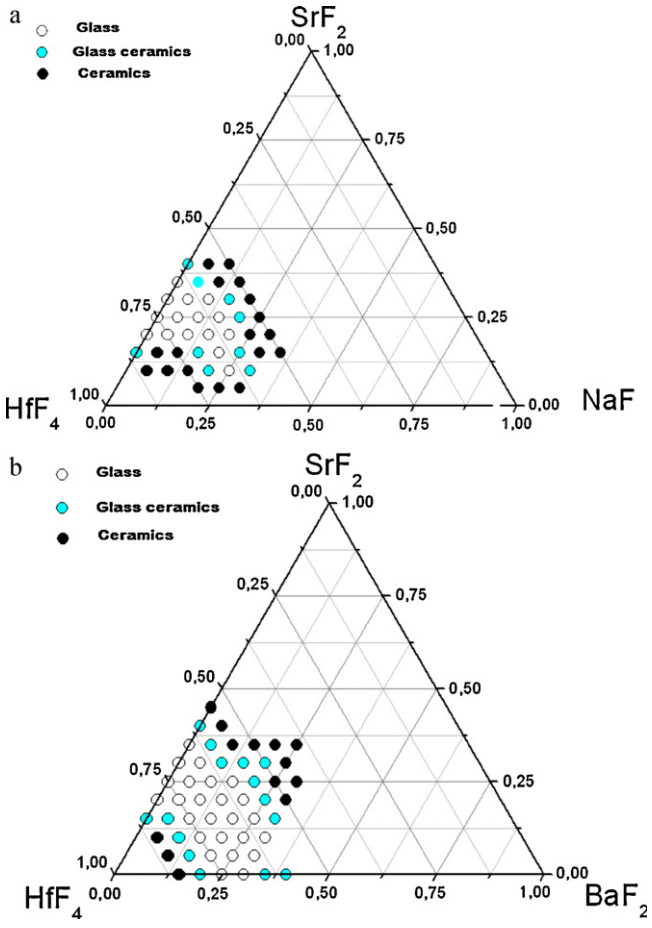

Fig. 6. Glass forming area in the HfF_4–SrF_2–NaF (a) and BaF_2 (b) ternary systems.

The search for extended IR transmission makes fluorohafnate glasses attractive. New glasses have been obtained in the HfF_4–SrF_2–MF_n (M = Na, Ca, Ba, La) ternary systems [19]. A typical vitreous diagram is shown in Fig. 6. High density fluorohafnate glasses could be used as scintillating materials for high energy physics and medical imaging.

Oxyfluoride glasses based on niobium oxyfluoride NbO_2F have been studied [20]. Among the aims of the work, one may quote the collection of new information about mechanism of glass formation, the decrease of the sensitivity to aqueous solutions and the increase of the refractive index and mechanical strength. Previous results have been completed by systematic investigations in the NbO_2F–BaF_2–MF (M = Li, Na, K) ternary systems [20]. Glass transition temperature is larger than that of fluorozirconates. It decreases as alkali content increases.

Fluorophosphate glasses have been synthesized by the incorporation of $NaPO_3$ leading to the MnF_2–$NaPO_3$–MF_n (M = Zn, Sr, Mg and Ba; Li, Na and K) [21]. Glass transition temperature is close to 250 °C and depends on composition. Main physical properties, including density, refractive index n_D, microhardness, and thermal expansion, have been measured. The incorporation of manganese fluoride at the expense of $NaPO_3$ leads to the increase of Tg, n_D, E (Young modulus) and microhardness, while chemical durability is enhanced. Optical transmission is limited in the UV spectrum by electronic transitions of Mn^{2+} ions in octahedral environment and in the IR spectrum by the P–O vibrations. Direct electrical conductivity and dependencies of complex electrical modulus versus temperature and frequency have been measured on glasses from the MnF_2–ZnF_2–$NaPO_3$ system [22]. These glasses are sensitive to atmospheric humidity. A corrosion layer is created by the effect of water and leads to the significant increase of the electrical conductivity in the case of $20ZnF_2$–$80NaPO_3$ glass. This behavior is governed by Arrhenius relation where the values of activation energy are increasing and values of the electrical conductivity are decreasing with the amount of MnF_2. This results from the predominant part of the Na^+ ionic conductivity that exceeds the electronic conductivity arising from glass defects. Sodium monofluophosphate Na_2PO_3F has been used to stabilize the NbO_2F–BaF_2-binary glasses [20]. Larger and thicker samples could be obtained in the NbO_2F–BaF_2–Na_2PO_3F ternary system, exemplifying the stabilization of the vitreous state. Their mechanical properties have been studied. NMR measurements show the evolution of the connectivity of the PO_4 tetrahedra versus composition. It has been shown that most tetrahedra are Q_0 and Q_1 type. In these conditions, the vitreous network consists in the associations of phosphate groups and $Nb(O,F)_6$ octahedra.

4. Conclusion

New heavy metal fluoride glasses compositions have been investigated, namely manganese-rich fluorozirconates and strontium fluorohafnates, in ternary systems such as ZrF_4–BaF_2–MnF_2 and HfF_4–SrF_2–BaF_2. Numerous fluorophosphate glasses have also been obtained by the incorporation of $NaPO_3$ and Na_2PO_3F in the unstable MnF_2–BaF_2 and NbO_2F–BaF_2 binary glasses. NMR and electrical conductivity measurements were conducted on these glasses.

(Er^{3+}/Ce^{3+} or Pr^{3+})-doped planar waveguides were made from the ZBLA glass used as a substrate. Channeled waveguide were obtained using optical lithography, SiO_2 mask and ion exchange method. The spectroscopic properties of Pr^{3+} doped waveguides were investigated by comparison to bulk samples with the same composition for the visible transition of interest ($^3P_0 \rightarrow {}^3H_4$ (blue), $^3P_1$, $^1I_6 \rightarrow {}^3H_5$ (green), $^3P_0 \rightarrow {}^3H_6$ (orange), $^3P_0 \rightarrow {}^3F_2$ (red)). Gain and optical losses measurement are currently under progress as well as the modelization of laser effect in Pr^{3+}-doped ZBLA matrix. In ZBLA waveguide co-doped with Cerium and Erbium, low background losses (0.3 dB/cm) and net gain in excess of 1 dB/cm were obtained at 1.54 μm for incident pump powers higher than 200 mW.

Acknowledgment

This work has been supported by French Research National Agency (ANR) through chemistry white program (project FLUOLASE).

References

[1] M. Poulain, J. Lucas, P. Brun, Mater. Res. Bull. 10 (1975) 243–246.
[2] A.E. Comyns, Chem. Br. 23 (1987) 563.
[3] I.D. Aggarwal, G. Lu, Fluoride Glass Fiber Optics, Academic Press Inc., Boston/New York/London, 1991.
[4] P. France, Fluoride Glass Optical Fibres, Blackie, Glasgow, 1990.
[5] M. Poulain, in: S. Ganapathy (Ed.), Fluoride Glasses: Properties, Technology and Applications, Research Signpost, Kerala, India, 2010.
[6] G. Mazé, in: A. Comyns (Ed.), Applications and Prospects, John Wiley & Sons, Chichester, 1989.
[7] X. Zhu, N. Peyghambarian, Adv. Optoelectron. 2010 (2010) 1–23.
[8] J.L. Adam, J. Non-Cryst. Solids 287 (2001) 401–404.
[9] G. Perrin, J. Woillez, O. Lai, J. Guerin, T. Kotani, P.L. Wizinowich, D. Le Mignant, M. Hrynevych, J. Gathright, P. Lena, F. Chaffee, S. Vergnole, L. Delage, F. Reynaud, A.J. Adamson, C. Berthod, B. Brient, C. Collin, J. Cretenet, F. Dauny, C. Deleglise, P. Fedou, T. Goeltzenlichter, O. Guyon, R. Hulin, C. Marlot, M. Marteaud, B.T. Melse, J. Nishikawa, J.M. Reess, S.T. Ridgway, F. Rigaut, K. Roth, A.T. Tokunaga, D. Ziegler, Science 311 (2006) 194.
[10] M. Bernier, D. Faucher, N. Caron, R. Vallee, Opt. Express 17 (2009) 16941–16946.
[11] M. Poulain, G. Maze, Chemtronics 3 (1988) 77–85.
[12] R. Sramek, G. Fonteneau, E. Josse, J. Lucas, J. Non-Cryst. Solids 256–257 (1999) 189–193.
[13] E. Josse, G. Fonteneau, J. Lucas, Mater. Res. Bull. 32 (1997) 1139–1146.

[14] H. Haquin, I. Vasilief, G. Fonteneau, V. Nazabal, J.-L. Adam, S. Guy, B. Jacquier, M. Couchaud, M. Rabarot, L. Fulbert, Optical Components and Materials, SPIE, San Jose, CA, (2004), pp. 23–28.
[15] H. Inoue, K. Soga, A. Makishima, J. Non-Cryst. Solids 325 (2003) 282–294.
[16] H. Yang, Z. Dai, J. Li, Y. Tian, J. Non-Cryst. Solids 352 (2006) 5469–5474.
[17] I. Vasilief, S. Guy, B. Jacquier, B. Boulard, Y.P. Gao, C. Duverger, H. Haquin, V. Nazabal, J.L. Adam, M. Couchaud, L. Fulbert, C. Cassagnettes, F. Rooms, D. Barbier, Appl. Opt. 44 (2005) 4678–4683.
[18] T. Djouama, A. Boutarfaia, M. Poulain, Optoelectron. Adv. Mater. Rapid Commun. 1 (2007) 122–128.
[19] S. Chaguetmi, A. Boutarfaia, M. Poulain, J. Non Oxide Glasses 2 (2010) 15–22.
[20] Z. Bouchaour, Thèse de Doctorat, Université de Rennes 1, 2007.
[21] T. Djouama, A. Boutarfaia, M. Poulain, J. Phys. Chem. Solids 69 (2008) 2756–2763.
[22] J. Kaluzny, M. Kubliha, V. Labas, T. Djouama, M. Poulain, J. Non-Cryst. Solids 355 (2009) 2003–2005.